The O−H Stretching $\Delta\nu = 3$, 4, and 5 Vibrational Overtones and Conformational Study of 2-Butanol

Shucheng Xu, Yonglin Liu, Guohe Sha, Cuohao Zhang, and Jinchun Xie*

State Key Laboratory of Molecular Reaction Dynamics, Dalian Institute of Chemical Physics, Dalian 116023, People's Republic of China

Received: April 21, 2000; In Final Form: July 6, 2000

The O−H stretching $\Delta\nu = 3$, 4, and 5 vibrational overtone spectra of 2-butanol (*sec*-butyl alcohol) in the gas phase are measured using cavity ring-down spectroscopy (CRDS), where two bands are observed for each vibrational level. They are assigned to the absorption of the O−H stretching vibrations of different conformations and further confirmed by density functional theory (DFT) calculations. The mechanical frequencies ω_e, anharmonicities $\omega_e\chi_e$, and dissociation energies D are evaluated by the local-mode theory. The band intensities of each band are obtained as well. The band shapes are simulated by a Lorentzian−Gaussian sum function. The molecular geometry, abundance, and O−H stretching frequencies of the calculated conformations are in good agreement with experimental results.

Introduction

Molecular conformation is an important aspect of stereochemistry. The compound 2-butanol (*sec*-butyl alcohol) is one of the typical alcohols with a stereo structure similar to those of ethanol and propanol.[1] Because the energy differences among different conformations of the molecule are small, resolving such differences by fundamental IR and Raman spectra is usually difficult.[2,3] However, optical overtone spectroscopy has higher resolving power for different molecular conformations because of the sensitivity of the overtone vibration to the local environment of X−H oscillators (X = C, N, O).[4] Meanwhile, for higher frequency, the overtone experiment can also be used to obtain information on molecular conformations that change on a time scale much shorter than the conventional NMR time scale.[5] Fang et al.[6] have studied successfully the molecular conformers of gas-phase ethanol by its vibrational overtones. Wong et al.[7] have studied the molecular conformation of alkanes and alkenes in the gas phase by overtone spectroscopy. They found, for a CH bond length change of 0.001 Å, a frequency shift of 69 cm^{-1} for the CH stretching $\Delta\nu_{CH} = 6$ overtone spectrum as compared to a frequency shift of 10 cm^{-1} for the fundamental. For the detection of even very weak absorptions by means such as overtone spectroscopy, techniques including photoacoustic laser spectroscopy,[8] long-path absorption spectroscopy,[9] and thermal-lens spectroscopy[10−12] have been used in the past decades. Recently, the advanced cavity ring-down spectroscopy (CRDS) technique has also shown great advantage in measurements for the overtone spectroscopy of weak absorptions,[13] especially for that of of 2-propanol and *iso*-butanol.[14,15] Furthermore, it yields absolute quantitative spectroscopic measurements.[16,17]

For overtones of 2-butanol, the O−H stretching $\Delta\nu = 2$, 3, 5, and 6 overtones in the liquid phase were measured in low resolution by means of the thermal-lens technique,[12,18] and the O−H stretching $\Delta\nu = 5$ overtone in the gas phase was measured roughly by an intracavity dye-laser photoacoustic spectrometer.[19] For conformational studies of this molecule, the total and relative energies of the gauche O−C−C−Me and anti O−C−C−Me conformations were calculated using restricted Hatree Fock (RHF) theory with the 3-21G and 6-31G* basis sets and single-point second-order Møller−Plesset (MP2) theory with the 6-31G* basis set.[20] The two-dimensional conformational energy maps for internal rotation of dihedral angles C−C−C−C and C−C−O−H were calculated using MM3 calculations, and only three stable conformers were discussed.[3] In this article, we report higher-resolution overtone spectra of the O−H stretching $\Delta\nu = 3$, 4, and 5 vibrations of 2-butanol in the gas phase using the highly sensitive CRDS technique and full information for nine stable molecular conformations calculated by highly accurate DFT theory at the Becke3LYP/6-31G* level.

Experimental Section

The CRDS experimental setup is similar to that used in our previous works.[14,15,17] The ring-down cavity is formed by two high-reflection concave mirrors with a diameter of 25 mm and a radius of curvature of −1 m, placed at a distance of slightly less than 1 m. The mirrors are connected through bellows with a glass cell, which is filled with pure molecular sample at a pressure of 15 Torr. A Nd:YAG laser-pumped (Precision, Continuum) pulsed OPO laser system (Sunlite, Continuum) runs at 10 Hz and in the range of 940−960 nm. Another excimer laser-pumped (EMG103, Lambda Physik) pulsed dye laser (FL2002, Lambda Physik) runs at 10 Hz and in the range of 720−750 nm when pumped by rhodamine 700 and 590−620 nm when pumped by rhodamine B. The laser light transmitted through the cavity is monitored using a photomultiplier tube (PMT), placed close behind the cavity. The ring-down signal from the PMT is digitized on a digital oscilloscope (LeCroy, 9350CM) with a 500-MHz sampling rate. The data are transferred into a computer via a GPIB interface connection. The characteristic ring-down time is determined by fitting the natural logarithm of the ring-down exponential decay to a straight line and by using a weighted least-squares fitting algorithm. We averaged the ring-down time for each laser shot instead of averaging the decay curve. At each wavelength, we

* Author to whom correspondence should be addressed. E-mail: xiejch@gingko.dlut.edu.cn.

10.1021/jp001529l CCC: $19.00
Published on Web 09/01/2000

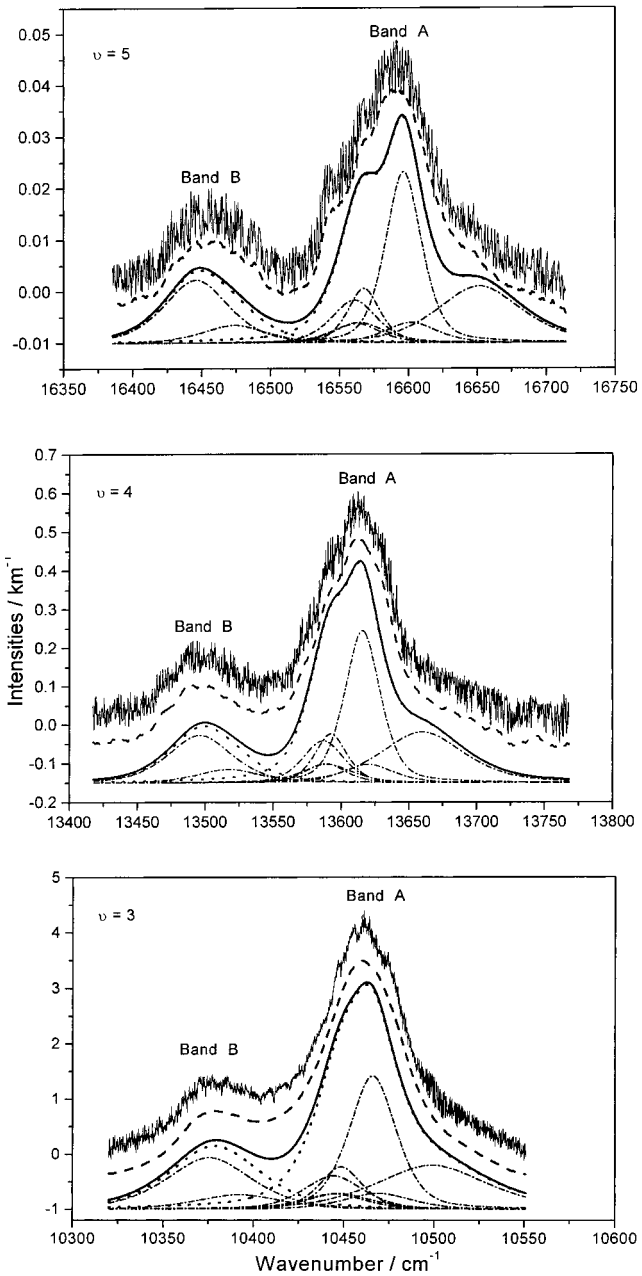

Figure 1. O−H stretching $\Delta\nu = 3$, 4, and 5 overtone spectra measured by CRDS for 2-butanol. The dashed curves are smoothed spectra, the solid curves are simulated spectra, the dotted curves are simulated two bands, and the dash-dotted curves are simulated spectra of each conformation by the sum of Lorentzian-Gaussian function.

averaged 10 times. The empty cavity ring-down times in our setup are about 1.5, 3, and 9 μs, respectively, for the wavelength ranges of 944−960, 725−740, and 595−610 nm, which correspond to mirror effective reflection coefficients of 0.9978, 0.9989, and 0.9996, respectively.

The purity of racemic 2-butanol (99.5%, Shanghai First Chemical Company) was verified by GC runs.

Results and Discussion

A. Spectroscopic Analysis of Overtones. The O−H stretching $\Delta\nu$ =3, 4, and 5 overtone spectra of 2-butanol are shown in Figure 1, where two resolved vibrational bands, A and B, are found for each overtone transition. The A and B bands have different band shapes, but they are almost identical in the $\Delta\nu = 3$, 4, and 5 spectra. The tendency of separation increases with the vibrational level ν. The band origins are measured by fitting the band shapes and calibrated by the standard water lines in the Hitran database 1996.[21] The values of the band origins of the O−H stretching $\Delta\nu = 5$ overtone listed in Table 1 are the same as those in ref 19, but a weak unassigned band at 16 372 cm^{-1} in the spectrum of ref 19 is not observed in this work. Shifted frequencies due to hydrogen bonding in the pure liquid phase have also been reported.[12,18]

The band intensities of the O−H stretching vibrations are also obtained from the CRD spectra. The band intensity formula for CRD absorption spectra[15] is expressed as

$$S_n = \frac{1}{P}\int \frac{1}{c}\left(\frac{1}{\tau} - \frac{1}{\tau_0}\right) \mathrm{d}\bar{\nu} \qquad (1)$$

with units of cm^{-1} km^{-1} atm^{-1}, where P is the sample pressure, room temperature $T = 300$ K, c is the speed of light, τ is the ring-down time with molecular absorption, $\tau_{0\ \mathrm{is}}$ the ring-down time at the off-resonance baseline, and $\bar{\nu}$ is the frequency. The experimental band intensities of the overtones are determined by the integrated area of the whole band shape, obtained by extending the fitted band shapes, as shown in Figure 1. Comparing the band intensities of the different vibrational levels in Table 1, the $\Delta\nu = 3$ overtone is 10 times stronger than $\Delta\nu = 4$, and the $\Delta\nu = 4$ overtone is almost another 10 times stronger than $\Delta\nu = 5$. The relative ratio for the band intensities of band A and band B are near 3:1 for the different vibrational levels.

Because the O−H stretch in alcohols is, to a very good approximation, nearly a local mode,[15,22] each band in the overtone spectra is assigned to the O−H stretching vibration. Therefore, O−H anharmonic oscillators can be treated by the Birge−Sponer equation[23]

$$\Delta E_{\nu,0} = \nu(A + B\nu) \qquad (2)$$

where $\Delta E_{\nu,0}$ is the observed energy difference between the νth quantum level and the ground state, $\omega_e = A - B$ is the mechanical frequency, $\omega_e\chi_e = -B$ is the anharmonicity, and $D = -A^2/4B$ is the dissociation energy. The ω_e, $\omega_e\chi_e$, and D values of the O−H stretching vibration for the A and B bands evaluated from the above spectra are listed in Table 1. The corresponding three parameters of the O−H stretching vibrations of 2-butanol in the gas phase are evidently different from their values for the liquid phase in ref 18, but these parameters are nearly identical with those of other alcohols in the gas phase such as methanol,[24,25] ethanol,[6] 2-propanol,[14] and *iso*-butanol,[15] which are $\omega_e = 3792-3855$ cm^{-1}, $\omega_e\chi_e = 83-86$ cm^{-1}, and $D = 117-119$ kcal mol^{-1}. Therefore, we can conclude that the O−H vibration in alcohols fits into the local mode in general. The obvious cleavage bands of the O−H vibration and the asymmetric band shapes of band A and band B should result from molecular geometric structure, namely, the different conformations of 2-butanol.

B. DFT Calculations of Molecular Conformations. The 2-butanol molecule exhibits different conformations because the functional group −OH bond staggers between the C−H bond and the $-CH_3$ group and the $-CH_2CH_3$ group rotates around the C−C single bond.[26] There were several conformational energy minima shown in the two-dimensional energy map for internal rotation of dihedral angles C−C−C−C, C−C−O−H using MM3 calculations.[3] To more accurately calculate these different conformations of the molecule, DFT calculations are performed with the Gaussian 98 programs.[27] All possible

TABLE 1: Observed Band Origins, Band Intensities, Mechanical Frequencies ω_e, Anharmonicities $\omega_e\chi_e$, and Dissociation Energies D for the O−H Stretching Overtones of 2-Butanol

molecule		$\nu_{OH}=3$		$\nu_{OH}=4$		$\nu_{OH}=5$				
band[a]	conformation[b]	band origin (cm^{-1})	S_n[c]	band origin (cm^{-1})	S_n	band origin (cm^{-1})	S_n	ω_e (cm^{-1})	$\omega_e\chi_e$ (cm^{-1})	D (kcal/mol)
band A	form a form b form c form d form e form f form g	10 461	13 680	13 614	1930	16 590[d]	187	3826 ± 2	−84.5 ± 1.0	118.4 ± 1.0
band B	form h form i	10 378	4256	13 497	557	16 449[d]	56	3798 ± 2	−84.8 ± 0.4	116.2 ± 1.0

[a] See Figure 1. [b] See Figure 2. [c] S_n band intensity in unit of cm^{-1} km^{-1} atm^{-1}. [d] The bands were also measured in ref 19.

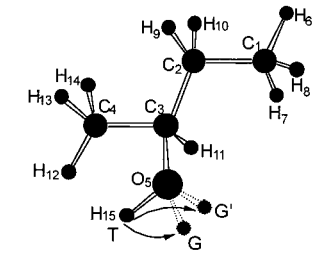

(a) $C_1C_2C_3C_4$ *trans* conformations

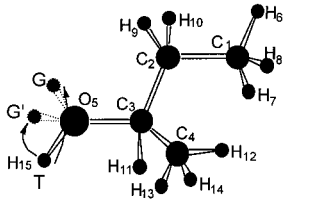

(b) $C_1C_2C_3O_5$ *trans* conformations

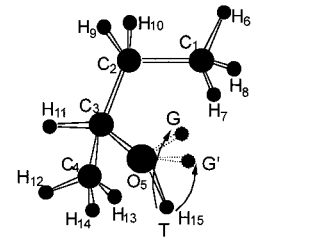

(c) $C_1C_2C_3H_{11}$ *trans* conformations

Figure 2. The nine stable conformations of 2-butanol: (a) $C_1C_2C_3C_4$ trans conformations [form a, *gg′t* (*g′gt*); form c, *gtt* (*g′tt*); and form i, *ggt* (*g′g′t*)]; (b) $C_1C_2C_3O_5$ trans conformations [form d, *ttg′* (*ttg*); form g, *tg′g′* (*tgg*); and form h, *tg′g* (*tgg′*)]; and (c) $C_1C_2C_3C_{11}$ trans conformations [form b, *g′tg* (*gtg′*); form e, *g′g′g* (*ggg′*); and form f, *g′gg* (*gg′g′*)].

conformations of 2-butanol are optimized using the B3LYP/6-31G* theory methods,[28,29] and their corresponding frequencies are also calculated. The possible conformations of 2-butanol can be named according to different angles of dihedral angles $C_1C_2C_3O_5$, $C_2C_3O_5H_{15}$, and $C_1C_2C_3C_4$, where trans (*t*) is 180°, gauche (*g*) is 60°, and gauche′ (*g′*) is −60°, respectively. The conformations of forms a, *gg′t* (*g′gt*); b, *g′tg* (*gtg′*); c, *gtt* (*g′tt*); d, *ttg′* (*ttg*); e, *g′g′g* (*ggg′*); f, *g′gg* (*gg′g′*); g, *tg′g′* (*tgg*); h, *tgg′* (*tg′g*); and i, *ggt* (*g′g′t*) in Figure 2 are all stable, because all of the fundamental frequencies of each conformer are real numbers. The conformational conformers in parentheses are mirror images of the corresponding conformers out of the parentheses because of the chirality of the molecule. The populations of these mirror images (named conformational enantiomers), and hence of exactly equal stability are, of course, equal.

The optimized geometries of the nine forms are listed in Table 2. The calculated values for the nine forms at the B3LYP/6-31G* level are as follows: bond lengths r_{CC} = 1.529−1.540 Å, r_{OC} = 1.431−1.433 Å, r_{HC} = 1.095−1.105 Å, and r_{HO} = 0.969−0.977 Å, and bond angles ∠COH = 107.1−107.8° ∠CCH (methylene) = 108.8−110.1°, and ∠CCO = 105.7−106.7° (HOCC trans) and 110.5−111.7° (HOCC gauche). These values are in good agreement with the experimental microwave data of methanol[30] and ethanol,[31] which are r_{CC} = 1.5297 Å, r_{OC} = 1.4246−1.4273 Å, r_{HC} = 1.0936 Å, and r_{HO} = 0.9451 Å; and ∠COH = 108.5°, ∠CCH (methylene) = 110.3°, and ∠CCO = 107.3° (HOCC trans) and 112.3° (HOCC gauche). Comparing calculated values of different forms, changes of CC bond lengths are less than 0.012 Å, and changes of other bond lengths are less than 0.004 Å. There are about 1−1.5° changes for bond angles ∠CCC among the different dihedral angle CCCC forms, where $\angle C_1C_2C_3$ = 113.5−113.8° (CCCC trans) and 114.4−115.1° (CCCC gauche), and $\angle C_2C_3C_4$ = 112.3−112.6° (CCCC trans) and 113.6−114.1° (CCCC gauche). For the different dihedral angle HOCC forms, the bond angles ∠CCO of the HOCC trans forms are less by about 5° than those of the HOCC gauche forms. Changes in the other bond angles among different conformations are less than 1°.

The calculated total energies, OH atomic charges, O−H stretching vibrational frequencies, and IR intensities for the molecular conformations are listed in Table 3. The calculated vibrational frequencies are scaled by factors of 0.977 for the B3LYP/6-31G* level, because of neglected anharmonicity and electron correlation.[32−34] According to thermodynamics, the lower the total energy of conformation, the more stable the conformation becomes. The total energy of form i is the lowest of the forms, and relative energies for forms a−h compared to that of i are 0.32, 1.31, 0.18, 0.91, 1.15, 1.42, 0.83, 0.79 kcal mol^{-1}, respectively. Therefore, the stability order of the nine forms should be form i > form c > form a > form h > form g > form d > form e > form b > form f. Generally, the $C_1C_2C_3C_4$ trans conformations are 0.4−0.9 kcal mol^{-1} more stable than the $C_1C_2C_3O_5$ trans conformations, and the $C_1C_2C_3O_5$ trans conformations are 0.3−0.6 kcal mol^{-1} more stable than the $C_1C_2C_3H_{11}$ trans conformations. Compared with previous calculated results, the $C_1C_2C_3C_4$ trans conformations are 0.8 kcal mol^{-1} (calculated by RHF/6-31G* and MP2/6-31G* in ref 20) or 0.5 kcal mol^{-1} (calculated by MM3 in ref 3) higher in energy than the $C_1C_2C_3O_5$ trans conformations. The energies of all of the conformations are closed to each other, and hence, the molecule can exist in any form under normal conditions. The relative percentage of the abundance of the molecular

TABLE 2: Optimized Geometry for 2-Butanol[a]

coordinate[b]	form a	form b	form c	form d	form e	form f	form g	form h	form i
$r(C_2-C_1)$	1.533	1.533	1.531	1.532	1.532	1.534	1.533	1.533	1.531
$r(C_3-C_{2)}$	1.536	1.534	1.529	1.531	1.540	1.541	1.536	1.536	1.536
$r(C_4-C_{3)}$	1.524	1.531	1.530	1.530	1.525	1.531	1.524	1.530	1.530
$r(O_5-C_{3)}$	1.432	1.432	1.432	1.431	1.433	1.431	1.431	1.431	1.432
$r(H_6-C_{1)}$	1.095	1.096	1.096	1.096	1.096	1.095	1.096	1.096	1.096
$r(H_7-C_{1)}$	1.097	1.096	1.097	1.096	1.096	1.096	1.095	1.096	1.094
$r(H_8-C_{1)}$	1.098	1.094	1.094	1.097	1.095	1.097	1.097	1.097	1.097
$r(H_9-C_{2)}$	1.099	1.097	1.098	1.097	1.101	1.097	1.101	1.097	1.099
$r(H_{10}-C_{2)}$	1.098	1.098	1.098	1.098	1.099	1.099	1.098	1.102	1.102
$r(H_{11}-C_{3)}$	1.105	1.104	1.105	1.105	1.104	1.097	1.105	1.098	1.098
$r(H_{12}-C_{4)}$	1.094	1.098	1.098	1.098	1.094	1.095	1.094	1.095	1.095
$r(H_{13}-C_{4)}$	1.096	1.095	1.096	1.096	1.095	1.098	1.095	1.096	1.099
$r(H_{14}-C_{4)}$	1.096	1.097	1.096	1.096	1.096	1.096	1.096	1.099	1.096
$r(H_{15}-O_{5)}$	0.969	0.970	0.970	0.970	0.970	0.970	0.970	0.971	0.972
$\angle(C_1C_2C_{3)}$	113.83	114.94	113.48	114.39	114.81	115.06	114.66	114.81	113.36
$\angle(C_2C_3C_{4)}$	112.30	114.09	112.48	113.64	114.09	113.97	113.67	113.78	112.55
$\angle(C_2C_3O_{5)}$	111.72	106.61	106.67	105.73	111.46	111.52	110.59	110.48	111.47
$\angle(C_2C_1H_{6)}$	111.20	110.51	111.05	110.67	110.80	110.67	110.89	110.85	111.32
$\angle(C_2C_1H_{7)}$	111.44	112.05	111.11	112.07	111.80	112.30	111.75	112.02	110.60
$\angle(C_2C_1H_{8)}$	111.46	110.61	110.63	111.34	110.61	111.22	111.30	111.11	110.98
$\angle(C_1C_2H_{9)}$	109.39	109.23	109.93	109.78	109.20	109.02	108.82	109.78	110.14
$\angle(C_1C_2H_{10)}$	109.71	110.24	110.08	110.34	110.30	109.63	110.45	109.60	109.90
$\angle(C_2C_3H_{11)}$	108.35	107.36	108.36	108.29	107.51	107.55	108.39	108.55	108.96
$\angle(C_3C_4H_{12)}$	110.35	110.63	110.99	110.81	109.96	110.00	109.91	110.01	110.35
$\angle(C_3C_4H_{13)}$	110.18	111.08	111.26	111.74	110.94	111.47	111.33	111.92	110.75
$\angle(C_3C_4H_{14)}$	110.87	111.16	110.30	110.21	110.73	111.31	110.27	110.65	111.38
$\angle(C_3O_5H_{15)}$	107.75	107.65	107.66	107.60	107.51	107.35	107.53	107.07	107.05
τ $(C_4C_3C_2C_{1)}$	179.39	61.22	177.16	66.10	61.18	64.56	65.17	64.21	−177.28
τ $(O_5C_3C_2C_{1)}$	60.20	−61.82	61.07	−172.27	−59.10	−62.13	−175.92	−170.58	57.35
τ $(H_6C_1C_2C_{3)}$	177.91	174.92	179.18	176.26	173.08	177.31	175.38	175.72	−176.94
τ $(H_7C_1C_2C_{3)}$	−62.87	−65.43	−60.99	−63.92	−67.05	−62.75	−64.73	−64.27	−56.25
τ $(H_8C_1C_2C_{3)}$	57.95	55.17	58.79	56.75	53.00	58.55	55.691	56.24	63.03
τ $(H_9C_2C_3C_{4)}$	−58.60	−177.12	−60.70	−171.92	−176.84	−173.79	−173.34	−173.53	−54.39
τ $(H_{10}C_2C_3C_{4)}$	57.08	−62.44	54.63	−57.43	−62.76	−58.69	−58.63	−58.85	60.41
τ $(H_{11}C_3C_2C_{1)}$	−60.44	−178.91	−56.78	54.54	−178.93	−175.38	−55.69	−57.18	−56.50
τ $(H_{12}C_4C_3C_{2)}$	−179.92	177.65	179.07	178.12	177.93	177.84	176.53	177.53	−179.05
τ $(H_{13}C_4C_3C_{2)}$	−60.58	−62.60	−61.21	−62.36	−62.79	−62.56	−63.35	−61.98	−59.36
τ $(H_{14}C_4C_3C_{2)}$	59.62	58.42	59.39	58.55	57.96	57.58	57.40	58.10	60.31
τ $(H_{15}O_5C_3C_{2)}$	−64.29	178.60	177.44	−179.01	−57.39	71.22	55.56	−64.05	64.58

[a] Calculations using the B3LYP/6-31G* method. [b] See Figure 2 for the nine conformers; bond lengths are in angstroms, bond angles in degrees.

TABLE 3: Calculated Total Energies, Relative Energies, OH Atomic Charges, O−H Stretching Fundamental Frequencies, Percentages of the Conformations, and Experimental O−H Stretching Fundamental Frequencies of 2-Butanol

conformation[a]	total energy[b] (Hartree)	relative energy (kcal mol^{-1})	atomic charge (electrons)		O−H str. fr eq. (calc.)[c] (cm^{-1})	O−H str. IR inten. (km/mol)	percentage[d]	O−H str. freq. (exp.)[e] (cm^{-1})	O−H str. freq. (exp.)[f] (cm^{-1})
			O_5	H_{15}					
form a	−233.529 775	0.32	−0.627	0.391	3668.9	7	17	3657 ± 2 (A)	3627
form b	−233.528 212	1.31	−0.626	0.386	3659.0	7	4		
form c	−233.530 012	0.18	−0.624	0.385	3657.9	8	22		
form d	−233.528 854	0.91	−0.629	0.384	3652.1	6	6		
form e	−233.528 474	1.15	−0.623	0.385	3651.4	6	4		
form f	−233.528 031	1.42	−0.624	0.385	3651.1	6	3		
form g	−233.528 975	0.83	−0.628	0.384	3650.7	6	7		
form h	−233.529 028	0.79	−0.622	0.379	3633.3	6	8	3628 ± 2 (B)	
form i	−233.530 296	0.00	−0.618	0.380	3627.8	6	29		

[a] See Figure 2. [b] Total energies calculated by the B3LYP/6-31G* method. [c] Frequencies calculated by the B3LYP/6-31G* method and scaled by factors of 0.977. [d] Percentages of the conformations calculated by Boltzmann formula. [e] Frequencies derived from the spectral parameters ω_e and $\omega_e\chi_e$ by local-mode theory. [f] Experimental O−H stretching frequencies measured in dilute CCl_4 solution, see ref 2.

conformations follows the Boltzmann formula

$$\frac{N_i}{N_j} = \exp\left(-\frac{(E_i - E_j)}{kT}\right) \tag{3}$$

where (N_i/N_j) is the ratio of the two conformations; E_i and E_j are the total energies of the two conformations, respectively; and T is the room temperature of 300 K. From the calculated results, the percentages of the nine conformational forms from a to i are 17, 4, 22, 6, 4, 3, 7, 8, and 29%, respectively. The calculated O−H stretching frequencies of conformations decrease in order from a to i, and the frequencies from b to g are very close to each other. The O−H stretching frequency is related to the polarizabilty of the −OH group, which is influenced by the local environment. The sum of the O and H atomic charges has shown different values of 1.02 for form a, 1.01 for forms b−g, and 1.00 electrons for forms h and i.

C. Assignments and Simulations of the Overtones. Because the O−H stretching frequencies of the most conformations are very close to each other, the broad vibrational absorption at

TABLE 4: Calculated Band Origin, Mechanical Frequencies ω_e, Relative Integral Areas *A*, and Simulated Half-Widths *W* of Conformations of 2-Butanol

conformation[a]	calc. band origin[b] (cm^{-1}) $\nu_{OH}=3$	$\nu_{OH}=4$	$\nu_{OH}=5$	calc. ω_e[b] (cm^{-1})	relative A[c] (km^{-1} cm^{-1})	simulated W (cm^{-1})
form a	10 499	13 660	16 652	3838	0.27 (A)	65
form b	10 469	13 620	16 602	3828	0.06 (A)	40
form c	10 466	13 616	16 597	3827	0.35 (A)	28
form d	10 448	13 593	16 568	3821	0.10 (A)	25
form e	10 446	13 590	16 564	3821	0.06 (A)	35
form f	10 445	13 589	16 563	3820	0.05 (A)	35
form g	10 444	13 587	16 561	3820	0.11 (A)	35
form h	10 392	13 517	16 474	3803	0.22 (B)	50
form i	10 376	13 495	16 446	3797	0.78 (B)	50

[a] See Figure 2. [b] Band origins and ω_e values deduced from DFT-calculated fundamental frequencies and experimetnal $\omega_e\chi_e$ value, 84.65 cm^{-1}. [c] Relative integral areas of conformations calculated by the Boltzmann formula.

room temperature make the overtones of most conformations overlap heavily. The two main absorption bands A and B observed in the $\Delta\nu$ =3, 4, and 5 overtones are the common concentrations of the O−H stretching overtone excitation of all of the conformations. The fundamental frequencies of 3657 ± 2 and 3628 ± 2 cm^{-1} derived from the spectral parameters of bands A and B, respectively, are very close to the frequencies of forms c at 3657.9 cm^{-1} and i at 3627.8 cm^{-1}, respectively. Therefore, the O−H stretching absorption of form c with 22% of the population makes the primary contribution to band A, and the absorptions of forms a, b, and d−g also make relatively small contributions to band A. The O−H stretching absorption of form i with 29% of the population makes the primary contribution to band B, and the O−H stretching absorption of form h also makes a smaller contribution to band B. Therefore, the sum of the relative populations of the conformations assigned to band A is 63%, and the sum of the relative populations of the conformations assigned to band B is 37%. It is also of interest to compare the relative band intensities of bands A and B in the overtones with the relative populations of their assigned conformations. We have to assume that the overtone transition strengths are the same for the O−H oscillators in the different conformations. In Table 3, the calculated IR intensities of the conformations are 6−8 km/mol, which are quite close to each other. Indeed, the relative ratio for the band intensities of the two bands A:B are near 3:1 for the different vibrational levels, which are comparable to the ratios for their assigned conformations.

The different extents of the contributions of each conformation to the overtone absorptions have produced a special band shape for each band. The band shapes of the overtones can be simulated using a combination of Gaussian and Lorentzian band-shape functions for each conformation. An isolated O−H stretching absorption band is of Lorentzian form with a Gaussian perturbation imposed. The sum function of Gaussian and Lorentzian form can be used for fitting band shapes[35] and is as follows

$$F(\gamma) = \frac{A}{2W\sqrt{\pi/2}}\, e^{-2[(\gamma-\gamma_0)^2/W^2]} + \frac{2A}{\pi}\frac{W}{4(\gamma-\gamma_0)^2+W^2} \quad (4)$$

where A is the integral area of the band in km^{-1} cm^{-1}, W is the half-width of the band in cm^{-1}, γ_0 is the band origin in cm^{-1}, and γ is the frequency in cm^{-1}. For the parameters of the band-shape function $F(\gamma)$ of each conformation in the $\Delta\nu$ = 3, 4, and 5 vibrational levels listed in Table 4, using eq 2, the band origin γ_0 is derived from its DFT-calculated fundamental frequency and the average experimental value for $\omega_e\chi_e$, 84.65 cm^{-1}; the relative percentage of absorption integral area for each conformation is calculated by eq 3; and the integral areas of bands A and B are obtained from the experimental band intensities. The band-shape function, $F_A(\gamma)$ for band A is the sum of $F_a(\gamma)$ for form a, $F_b(\gamma)$ for form b, $F_c(\gamma)$ for form c, $F_d(\gamma)$ for form d, $F_e(\gamma)$ for form e, $F_f(\gamma)$ for form f, and $F_g(\gamma)$ for form g; $F_B(\gamma)$ for band B is the sum of $F_h(\gamma)$ for form h and $F_i(\gamma)$ for form i. The whole band-shape function $F(\gamma)$ is the sum of $F_A(\gamma)$ and $F_B(\gamma)$. As shown in Figure 1, the smoothed curves of the original spectra are fit by a band-shape function in which the simulated half-width W of each conformation for the different levels is kept the same. The simulated spectrum for the $\Delta\nu$ = 3 vibrations approaches the experimental spectrum, and the simulated bands B for the $\Delta\nu$ = 4 and 5 vibrations also approach the experimental spectra. However, the simulated bands A for the $\Delta\nu$ = 4 and 5 vibrations come out with two shoulders because of the presence of combined bands, which cannot completely reproduce the experimental bands A, because only a weak shoulder in the left of band A is observed. It is noticed that the parameters for the frequencies, relative populations, and integral areas of the bands in the simulated spectra are all from the calculated or experimental values; only simulated half-widths are variable parameters. Therefore, the small difference between the calculated and experimental values causes a slight difference between the simulated spectra and experimental spectra.

Conclusion

We have studied the O−H stretching $\Delta\nu$ = 3, 4, and 5 overtone spectra of 2-butanol by taking advantage of the CRDS technique. In the spectra, the resolved two bands are assigned as the absorptions of the O−H stretching vibration of the different conformations. The $\Delta\nu$ = 3, 4, and 5 overtones provide conclusive spectral parameters for the O−H vibration, which bridge the gap between experiment and theory. The present quantum chemistry DFT methods have calculated the nine stable conformational isomers of the molecule, and their O−H stretching fundamental vibrations. We found good agreement between theoretically calculated vibrational frequencies and those obtained from experiment. The relative percentages of the measured spectral band intensities also correspond to the abundance of the assigned conformations with a specific total energy. The band-shape function is given in the form of the sum of Lorentzian and Gaussian functions, and the simulated spectra in the O−H stretching $\Delta\nu$ = 3, 4, and 5 vibrations clearly show the contribution of each conformation to the bands of the overtones. In conclusion, the properties of the molecular conformations can be shown clearly by means of experimental CRD overtone spectroscopy and theoretical DFT calculations.

Acknowledgment. This work was supported by grants from the National Natural Science Foundation of China, Ministry of Science and Technology, and Chinese Academy of Sciences. J.C.X. also thanks the Hong Kong Qiu Shi Foundation, the Wang Kuancheng Foundation, and the San Francisco Li Foundation.

References and Notes

(1) Truax, D. R.; Wieser, H. *Chem. Soc. Rev.* **1976**, *5*, 411.
(2) Lutz, E. T. G.; van der Maas, J. H. *Spectrochim. Acta* **1978**, *34A*, 915.
(3) Hagemann, H.; Mareda, J.; Chiancone, C.; Bill, H. *J. Mol. Struct.* **1997**, *410−411*, 357.

(4) Crim, F. F. *Annu. Rev. Phys. Chem.* **1984**, *35*, 657.
(5) Henry, B. R. *Acc. Chem. Res.* **1987**, *20*, 429.
(6) Fang, H. L.; Swofford, R. L. *Chem. Phys. Lett.* **1984**, *105*, 5.
(7) Wong, J. S.; Moore, C. B. *J. Chem. Phys.* **1982**, *77*, 603.
(8) Quack, M. *Annu. Rev. Phys. Chem.* **1990**, *41*, 839.
(9) Stone, J. *Appl. Opt.* **1978**, *17*, 2876.
(10) Long, M. E.; Swofford, R. L.; Albrecht, A. C. *Science* **1976**, *191*, 183.
(11) Swofford, R. L.; Long, M. E.; Burberry, M. S.; Albrecht, A. C. *J. Chem. Phys.* **1977**, *66*, 664.
(12) Mizugai, Y.; Takimoto, F.; Katayama, M. *Chem. Phys. Lett.* **1980**, *76*, 615.
(13) Romanini, D.; Lehmann, K. K. *J. Chem. Phys.* **1995**, *102*, 663.
(14) Xu, S. C.; Zhang, L.; Dai, D.; Jiang, B.; Xie, J.; Sha, G.; Zhang, C. *Chin. J. Chem. Phys.* **2000**, *13*, 149−155.
(15) Xu, S. C.; Liu, Y.; Xie, J.; Sha, G.; Zhang, C., manuscript to be submitted.
(16) Zalicki, P.; Zare, R. N. *J. Chem. Phys.* **1995**, *102*, 2708.
(17) Xu, S. C.; Dai, D.; Xie, J.; Sha, G.; Zhang, C. *Chem. Phys. Lett.* **1999**, *303*, 171.
(18) Rai, S. B.; Srivastava, P. K. *Spectrochim. Acta* **1999**, *55A*, 2793.
(19) Jasinski, J. M. *Chem. Phys. Lett.* **1984**, *109*, 462.
(20) Houk, K. N.; Eksterowicz, J. E.; Wu, Y. D.; Fuglesang C. D.; Mitchell, D. B. *J. Am. Chem. Soc.* **1993**, *115*, 4170.
(21) The software Hitran 1996 was developed under Contract F19628-91-C-0132 for Phillips Laboratory Geophysics Directorate under the direction of Dr. Laurence Rothman, ONTAR Corporation, North Andover, MA.
(22) Zerbi, G.; Overend, J.; Swofford, R. L. *J. Chem. Phys.* **1968**, *38*, 122.
(23) Birge, R. T.; Sponer, H. *Phys. Rev.* **1926**, *28*, 259.
(24) Sage, M. L. *J. Chem. Phys.* **1984**, *80*, 286.
(25) Fang, H. L.; Meister, D. M.; Swofford, R. L. *J. Phys. Chem.* **1984**, *88*, 405.
(26) Csizmadia, I. G. *Molecular Structure and Conformation*; Elsevier Scientific Publishing Company: New York, 1982.
(27) Frisch, M. J.; Trucks, G. W.; Schlegel, H. B.; Scuseria, G. E.; Robb, M. A.; Cheeseman, J. R.; Zakrzewski, V. G.; Montgomery, J. A., Jr.; Stratmann, R. E.; Burant, J. C.; Dapprich, S.; Millam, J. M.; Daniels, A. D.; Kudin, K. N.; Strain, M. C.; Farkas, O.; Tomasi, J.; Barone, V.; Cossi, M.; Cammi, R.; Mennucci, B.; Pomelli, C.; Adamo, C.; Clifford, S.; Ochterski, J.; Petersson, G. A.; Ayala, P. Y.; Cui, Q.; Morokuma, K.; Malick, D. K.; Rabuck, A. D.; Raghavachari, K.; Foresman, J. B.; Cioslowski, J.; Ortiz, J. V.; Stefanov, B. B.; Liu, G.; Liashenko, A.; Piskorz, P.; Komaromi, I.; Gomperts, R.; Martin, R. L.; Fox, D. J.; Keith, T.; Al-Laham, M. A.; Peng, C. Y.; Nanayakkara, A.; Gonzalez, C.; Challacombe, M.; Gill, P. M. W.; Johnson, B. G.; Chen, W.; Wong, M. W.; Andres, J. L.; Head-Gordon, M.; Replogle, E. S.; Pople, J. A. *Gaussian 98*, Gaussian, Inc.: Pittsburgh, PA, 1998.
(28) Hehre, W. J.; Radom, L.; Schleger, P. V. R.; Pople, J. A. *Ab Initio Molecular Orbital Theory*; Wiley: New York, 1986.
(29) Foresman, J. B.; Frisch, M. J. *Exploring Chemistry with Electronic Structure Methods*, 2nd ed.; Gaussian, Inc.: Pittsburgh, PA, 1996.
(30) Lees, R. M.; Baker, J. G. *J. Chem. Phys.* **1968**, *48*, 5299 and references therein.
(31) Sasada, Y.; Takano, M.; Satoh, T. *J. Mol. Spectrosc.* **1971**, *38*, 33 and references therein.
(32) Johnson, B. G.; Gill, P. M. W.; Pople, J. A. *J. Chem. Phys.* **1993**, *98*, 5612.
(33) Xu, S.C.; Wang, C.; Sha, G.; Xie, J.; Yang, Z. Z. *J. Mol. Struct. (THEOCHEM)* **1999**, *459*, 163.
(34) Xu, S. C.; Wang, C.; Sha, G.; Xie, J.; Yang, Z. Z. *J. Mol. Struct. (THEOCHEM)* **1999**, *467*, 85.
(35) Pitha, J.; Jones, R. N. *Can. J. Chem.* **1966**, *44*, 3031.